

Neural Network-based Friction Identification in Hydraulic Actuators

Lőrinc Márton, Szabolcs Fodor

Dept. of Electrical Engineering
Sapientia Hungarian University of Transylvania
540485 Tîrgu Mureș, Op. 9, Cp 4, Romania
martonl@ms.sapientia.ro, f_szabi@yahoo.com

Abstract: The motion of hydraulic actuators are severely influenced by friction. In this paper the slip friction in hydraulic actuators is measured using a technique that was originally developed for electrical motor driven mechanical systems (see [1]). The method is based on pressure measurement made in constant velocity regimes. The value of the friction force for different velocity regimes was calculated using the measured chamber pressures. To describe the nonlinear nature of friction, feed-forward and radial basis function type neural networks have been applied for friction modeling. Real time experimental results are provided to show the applicability of the proposed identification strategy.

1 Introduction

Friction identification and modeling is the first step towards efficient friction compensation in mechanical control systems. In high precision position control systems the friction cannot be omitted during controller design [7]. The nonlinear nature of friction could have a negative influence on control characteristics; it can generate undesired effects such as limit cycle, steady state error or tracking lag.

Hydraulic actuators are widely used in many industrial systems such as heavy-duty manipulators or excavators. The walls and pistons of these actuators are lubricated with oil or grease (hydrodynamic lubrication). Tribological experiments showed that in the case of lubricated contacts in the low velocity regime the friction force decrease with velocity (Stribeck effect). In the high velocity regime the friction force increases with velocity (viscous friction). Both static [3] and dynamic [4] models were introduced to explain this phenomenon. One of the most common one is the exponential Stribeck model:

$$F_f = \begin{cases} \min(|u|, F_S) \text{sign}(u), & \text{for } v_p = 0 \\ \left(F_C + (F_S - F_C) e^{-|v_p|/v_s} \right) \text{sign}(v_p) + F_V v_p, & \text{otherwise} \end{cases} \quad (1)$$

where u denotes the tangential control force, v_p denotes the velocity. The parameters of the model are: $F_C > 0$ denotes the Coulomb friction coefficient, $F_S > 0$ is the static friction coefficient, $F_V > 0$ is the viscous friction coefficient, $v_S > 0$ is the Stribeck velocity. The friction can be described with switching model, since when the velocity is zero the machine does not start moving until the value of the control force reaches the level of the static friction.

To deal with friction in hydraulic actuators both identification and compensation algorithms were proposed. The paper [8] describes how the Coulomb and viscous friction coefficients, beside other dynamic parameters, can be identified in a hydraulically driven excavator using Least Squares and generalized Newton methods. A friction identification method was introduced in [3] for a parallel hydraulic actuator based on a simplified form of the model (1). With known or partially known friction parameters, control algorithms with friction compensation terms were introduced. In [2] a Lyapunov-based discontinuous friction compensation technique is developed for the position regulation of a hydraulic actuator using static friction model. In [6] the dynamic LuGre friction model was applied as friction compensator term in a hydraulic robot. Neural networks are also widely used to model the friction in hydraulic actuators. In [9] neural network based strategy was proposed for friction compensation. In [10] dynamic neural networks were applied for fault detection in hydraulically actuated rolling mills.

The rest of the paper is organized as follows: Section 2 presents the dynamic model of the hydraulic actuator that was used for identification. Section 3 details the characteristics and the parameters of the actuator and its control system using which the friction identification was performed. Section 4 presents the proposed friction measurement procedure, the neural network based identification method and the experimental results of the identification. Finally, Section 5 sums up the conclusions of this study.

2 Nonlinear Model of the Actuator

A schematic of a servo-valve controlled hydraulic actuator is shown in Figure 1. The mathematical model that relates the control input u to the output variable (the actuator position x_p) depends on the dynamics of the valve spool, the nonlinear flows through the valve control ports, the deformation and compressibility flows, as well as the Newtonian mechanics of the piston motion.

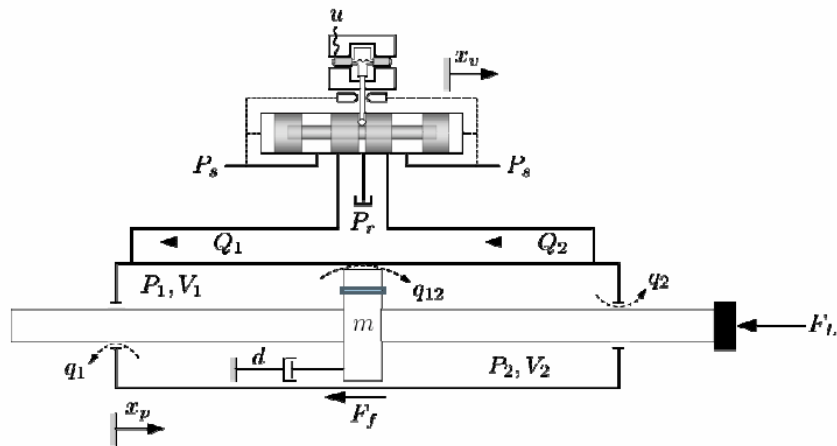


Figure 1

Schematic of hydraulic actuator for mathematical modeling

For a two-stage flapper-nozzle servo-valve, the relationship between the input current of the torque motor and the position of the valve spool is nonlinear. However, in the design of hydraulic servo-systems, detailed analysis of the non-ideal valve characteristics is generally not required. For control system design the servo-valve spool dynamics are often approximated using linear transfer function as model that captures the main characteristics of the valve dynamics in the low frequency range. Here, a second-order model is used to approximate the dynamics of the servo-valve spool position. A second order lag representation is generally adequate for the position servos since the servo-valve frequency response is well approximated to the point where the phase lag of the real valve is -90° . The relationship position of the valve spool x_v , and the current u , applied to the torque motor is:

$$x_v = -\frac{1}{\omega_v^2} \ddot{x}_v - \frac{2\zeta_v}{\omega_v} \dot{x}_v + k_v u \quad (2)$$

where k_v is the valve spool position gain and parameters ω_v and ζ_v are the natural frequency and the damping ratio that best represents the servo-valve magnitude and phase characteristics in the low frequency range. The values of this second-order model parameters can easily be estimated from valve frequency response curves given in manufacturer's catalogs.

For a valve with a critically-lapped spool having matched and symmetrical orifices, control flows Q_1 and Q_2 follows the turbulent orifice equation. The nonlinear governing equation can be written in the following compact form:

$$Q_2 = K_v \omega x_v \sqrt{\frac{P_s - P_R}{2} + \frac{x_v}{|x_v|} \left(\frac{P_s - P_R}{2} - P_1 \right)} \quad (3)$$

$$Q_2 = K_v \omega x_v \sqrt{\frac{P_s - P_R}{2} + \frac{x_v}{|x_v|} \left(P_2 - \frac{P_s - P_R}{2} \right)} \quad (4)$$

In equations (3) and (4), $K_v = C_v \sqrt{\frac{2}{\rho_{oil}}}$ is the valve flow gain, which depends on the orifice coefficient of discharge C_v and the density ρ_{oil} of the hydraulic fluid. Parameter ω is the width of the rectangular port cut into the valve bushing through which the fluid flows. The supply and tank pressures are denoted by P_s and P_r , respectively, while variables P_1 and P_2 refer to the hydraulic pressures in each of the actuator cylinders.

The continuity equations for compressible fluid volumes describe the time rate of change of the pressure in each actuator chamber. The continuity equation considers both the deformation and the compressibility flows and can be written for each cylinder half as:

$$\dot{P}_1 = \frac{\beta_h}{Ax_p - \bar{V}_1} (Q_1 - A\dot{x}_p) \quad (5)$$

$$\dot{P}_2 = \frac{\beta_h}{A(L - x_p) + \bar{V}_2} (-Q_2 + A\dot{x}_p) \quad (6)$$

In equations (5) and (6), A is the annulus areas of the piston; parameter β_h denotes the effective bulk modulus of the hydraulic fluid. The volumes of oil contained in the connecting lines between the servo-valve and actuator are given by \bar{V}_1 and \bar{V}_2 . The length of the actuator stroke is denoted by L .

In order to complete the mathematical model of the hydraulic servo-actuator, the Newtonian mechanics governing the motion of the actuator are now considered. By carrying out a force balance on the piston, it is found that the motion of the actuator can be described by the following equation:

$$m\ddot{x}_p + d\dot{x}_p = F_a - F_L - F_f \quad (7)$$

In (7) m is the combined mass of the piston, actuator rods and load, and parameter d is the equivalent viscous damping coefficient, which describes the combined effect of the viscous friction between the piston and the cylinder walls and the

damping load. $F_a = A(P_1 - P_2)$ is the force generated by the actuator, while force F_L refers to the external load disturbance. The force acting between the piston and the cylinder walls due to friction is denoted by F_f .

The nonlinear model of the entire hydraulic actuator in state space can be written based on equations (2) to (7).

$$\begin{cases} \dot{x}_p = v_p \\ \dot{v}_p = \frac{1}{m}(AP_1 - AP_2 - dv_p) - \frac{1}{m}F_d \\ \dot{P}_1 = \frac{\beta_h}{Ax_p - \bar{V}_1} \left[K_v \omega x_v \sqrt{\frac{P_s - P_R}{2} + \frac{x_v}{|x_v|} \left(\frac{P_s - P_R}{2} - P_1 \right)} - Av_p \right] \\ \dot{P}_2 = \frac{\beta_h}{A(L - x_p) + \bar{V}_2} \left[-K_v \omega x_v \sqrt{\frac{P_s - P_R}{2} + \frac{x_v}{|x_v|} \left(P_2 - \frac{P_s - P_R}{2} \right)} + Av_p \right] \\ \dot{x}_v = v_v \\ \dot{v}_v = -\omega_v^2 x_v - 2\zeta_v \omega_v v_v + k_v \omega_v^2 u \end{cases} \quad (8)$$

The nonlinear state equations (8) are valid for both extending and retracting strokes and the states v_p and v_v refer to the velocities of the piston and the valve spool. The output variable for position control is x_p and the two system inputs are the control valve command signal u , and the total disturbing force $F_d = F_L + F_f$.

3 The Experimental Setup

The experimental setup's schematic is shown in Figure 2. The entire system is powered by a motor driven hydraulic pump, which offers continuous and stable high-pressure hydraulic fluid (up to 18.27MPa, i.e. 2650psi) to the actuator.

The actuator is a double-rod cylinder with the parameters enumerated in Table 1. Since the actuator is symmetric and can actually move in either direction, the modelings of both chambers are identical. The two chambers are thus noted as chamber 1 and chamber 2. The actuator is connected to and controlled by a Moog D765 servo-valve (see Figure 2). This servo-valve receives control signals from a PC equipped with a DAS-16 data acquisition board and a Metrabyte M5312 encoder card. When operated at 20.7 MPa (3000psi), Moog D765 valve can supply the actuator with hydraulic fluid at a rate of 34L/min. During the experiments the operating pressure is set to approximately 13.8MPa (2000psi).

All the control strategies and experimental algorithms are implemented on a PC with an Intel Pentium III processor. The displacement of the actuator can be measured using Metrabyte M5312 quadrature incremental encoder card. With its rotary optical encoder, M5312 reaches a position measurement resolution of 0.03mm per increment. Other necessary system states are measured by transducers mounted on the hydraulic circuit and transmitted to the DAS-16 board; meanwhile the DAS-16 board also transmits control signals from the PC to the Moog D765 valve.

Table 1
List of nominal system parameters under normal operation

Supply pressure	P_s	$\leq 17 \text{ MPa}$
Tank pressure	P_R	$< 0.25 \text{ MPa}$
Mass of piston, rods and load	m	12.3 Kg
Viscous damping coefficient	d	$250 \text{ N} \cdot \text{sec}/\text{m}$
Piston annulus area	A	6.63 cm^2
Actuator stroke	L	6.96 cm
Line volumes	$\overline{V}_1, \overline{V}_2$	88.7 cm^3
Hydraulic density	ρ_{oil}	$847 \text{ kg}/\text{m}^3$
Fluid bulk modulus	β_h	689 MPa
Servo-valve discharge coefficient	C_v	0.6
Servo-valve flow gain	K_v	$2.92 \times 10^{-2} \text{ m}^{3/2} / \sqrt{\text{kg}}$
Maximum valve spool displacement	x_{vm}	$\pm 0.279 \text{ mm}$
Servo-valve orifice area gradient	ω	$20.75 \text{ mm}^2 / \text{mm}$
Servo-valve spool position gain	k_v	$0.0279 \text{ mm}/\text{V}$
Servo-valve natural frequency	ω_v	175 Hz
Servo-valve damping ratio	ζ_v	0.65 cm^3

4 Friction Measurement

The friction depends on velocity; hence it should be measured for different constant velocity values. In the other hand the frictional parameters may differ for positive and negative velocity domains, the measurement should be performed in both velocity domains separately.

According to (7), the friction force is proportional with the actuator force if the velocity is kept constant and there is no external load on the actuator:

$$F_a = F_f(v) \quad (9)$$

Note that the viscous coefficient in (7) is incorporated into the friction force.

The actuator force is given by:

$$F_a = A(P_1 - P_2) \quad (10)$$

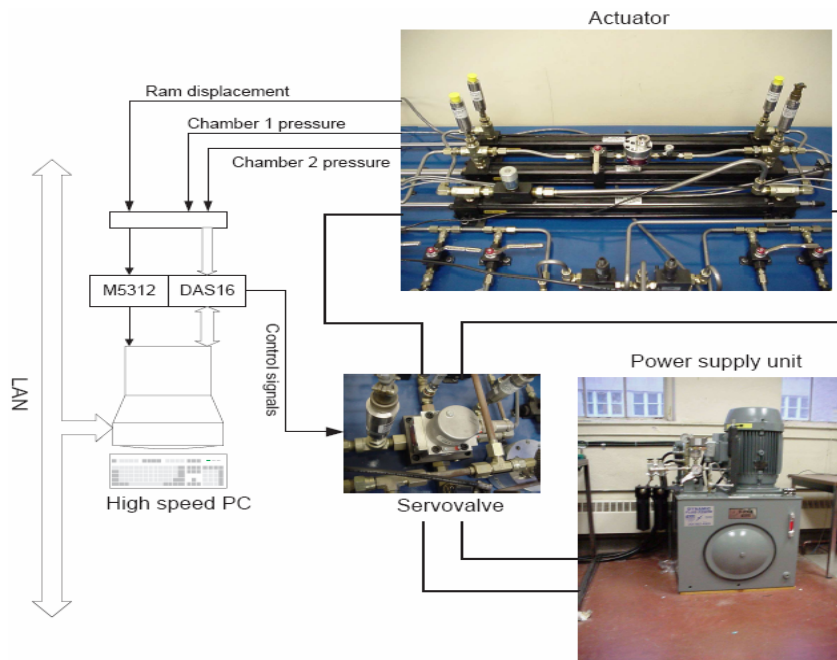


Figure 2
Hydraulic test rig with its interfacing

The measurement algorithm can be summarized as follows:

- Stabilize the velocity to v_i .
- After the transients, set the average of the velocity and the pressures in the chambers over a given time period to get rid of measurement noise.
- Calculate the friction force using (9), (10).
- Save the measurement data (v_i, F_{fi}).
- Repeat the sequence for the next velocity v_{i+1} .

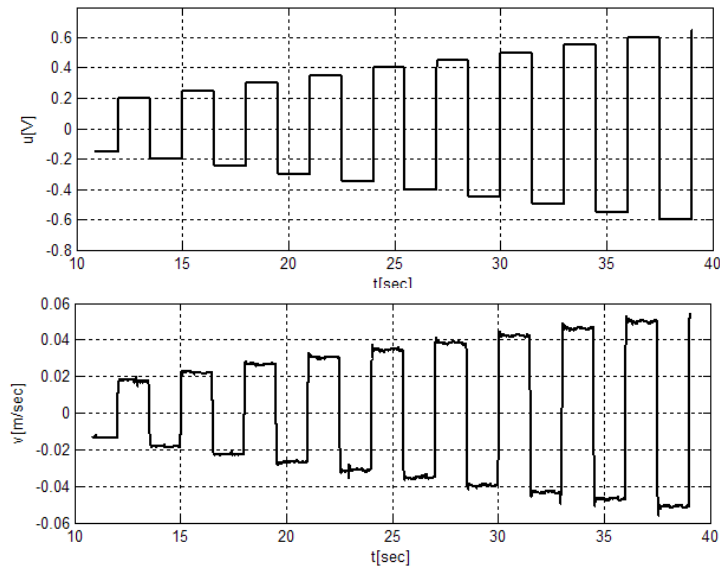


Figure 3

Control input and the actuator velocity during identification

To implement the algorithm, a square control signal (u) was applied for the actuator for 150 seconds. The amplitude of the control signal was increased with a 0.05 V step in every period, see Figure 3.

In Figure 4 and Figure 5 one measurement period can be seen constant velocity regimes and constant actuator force regimes are shown for both positive and negative domains. To get rid of measurement noise the pressure signals were filtered. The difference between the filtered and unfiltered signals can be seen in the Figure 5. The parts of the signals based on which the measurement point was determined by average calculation are marked with red on the figures.

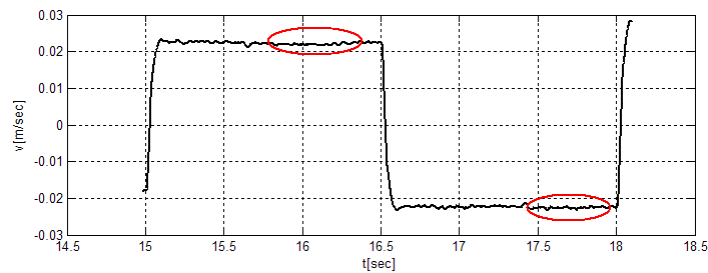


Figure 4

Velocity domains to capture a measurement point

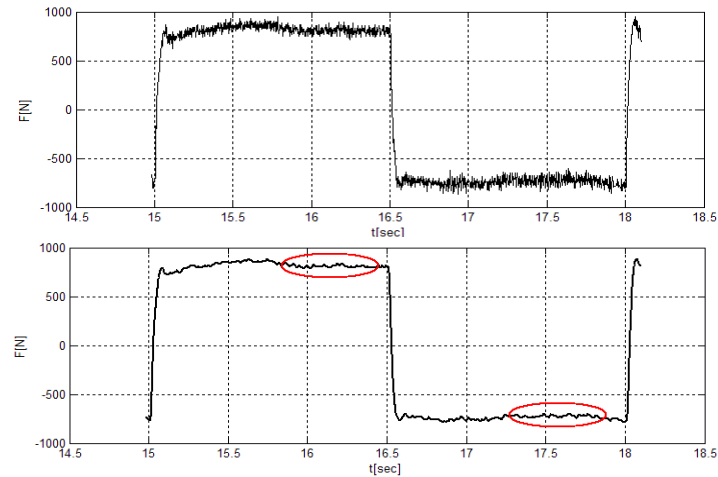


Figure 5

Friction force domains to capture a measurement point (unfiltered and filtered)

5 Neural Network-based Identification

Neural network based identification methods are frequently used for nonlinear curve fitting and function approximation problems. Neural networks are capable for precise approximation but this type of identification requires a more complex computational structure.

For the approximation two types of neural networks are proposed: feed-forward network and Radial Basis Function network. The inputs of the neural networks are the velocity of the actuator, the training set is given by the measurement points.

The feed forward network was created with the help of the ‘newff’ MATLAB function. This network has two layers; the first one contains 10 neurons, while the second output layer 1 neuron. For learning, the Levenberg – Marquadt training method and the Mean Square Error performance goal was applied. The curve approximation in the case of the feed-forward network is shown in Figure 7a.

The fitting error is given by:

$$E = \frac{1}{N} \left(\sum_{i=1}^N |F_f(v_i) - F_{fNN}(v_i)| \right) \quad (11)$$

where $F_{fNN}(v)$ is the neural network output vector.

In the case of the feed-forward network the value of the error was found as: $E = 3.0787$.

The Radial Basis Function network was created with the help of ‘*newrb*’ MATLAB function with 50 neurons in the hidden layer. According to (11) the fitting error was determined (see Figure 6d) and its value was found as $E = 2.4838$. The approximation of the friction curve can be seen in Figure 6c.

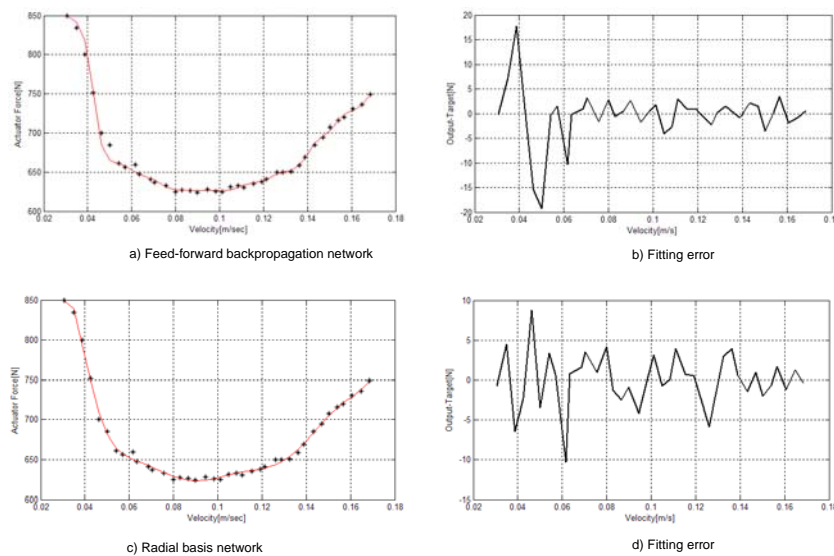


Figure 6
Neural network based identification

Conclusions

A friction measurement and identification algorithm was proposed for hydraulic actuators. The friction measurement method is based on chamber pressure and measurement and it explores that the complex nonlinear mathematical model of the hydraulic actuator reduces to a simple form if the velocity of the piston is constant. Neural network models were applied to approximate the measured friction characteristic. Experimental results shows that the proposed measurement and identification method captures precisely the nonlinear nature of friction hence it can effectively be applied for friction modeling and compensation.

Acknowledgement

The authors would like to thank Prof. Nariman Sepehri, University of Manitoba, Winnipeg for allowing the authors to perform the friction measurements in his laboratory, and for his usfull comments and remarks.

The first author research was supported by the János Bolyai Research Scholarship of the Hungarian Academy of Sciences and by the Hungarian National Research program under grant No. OTKA K 71762.

References

- [1] Lőrinc Márton, Béla Lantos, Friction and backlash measurement and identification method for robotic arms IEEE International Conference on Advanced Robotics, München, Germany, June 22 -26, 2009
- [2] P. Sekhavat, Q. Wu and N. Sepehri, Lyapunov-based Friction Compensation for Accurate Positioning of a Hydraulic Actuator, in Proceeding of the 2004 American Control Conference Boston, Massachusetts, June 30 - July 2, 2004
- [3] B. Armstrong-Helouvry, Control of Machines with Friction, Kluwer Academic Press, Boston, 1991
- [4] Carlos Canudas de Wit, H. Ollson, K. J. Astrom and P. Lischinsky, A new model for control of systems with friction, *IEEE Trans. on Automatic Control*, Vol. 40, No. 3, 1995, pp. 419–425
- [5] Zakarya Zyada and Toshio Fukuda, Identification and Modeling of Friction Forces at a Hydraulic Parallel Link Manipulator Joints, Proc. of 40th SICE Annual Conference, Nagoya, July 25-27, 2001
- [6] P. Lischinsky, C. Canudas de Wit and G. Morel, Friction compensation of a Schilling Hydraulic Manipulator, in Proc. of 1997 IEEE International Conference on Control Applications, Hartford, CT, October 5-7, 1997
- [7] Adrian Bonchis, Peter I. Corke and David C. Rye, Experimental Evaluation of Position Control Methods for Hydraulic Systems, *IEEE Transactions on Control Systems Technology*, Vol. 10, No. 6, November 2002, pp. 876-882
- [8] Y. H. Zweiri, L. D. Seneviratne and K. Althoefer, Identification Methods for Excavator Arm Parameters, in Proc. of SICE Annual Conference in Sapporo, August 4-6, 2004
- [9] S. B. Choi, C. C. Cheong, J. M. Jung and Y. T. Choi Position control of an ER Valve-Cylinder System Via Neural Network Ccontroller, *Mechatronics* Vol. 7, No. 1, 1997, pp. 37-52
- [10] Teodor Marcu, Birgit Koppen-Seligerb, Reinhard Stucher, Design of fault detection for a hydraulic looper using dynamic neural networks, *Control Engineering Practice* 16, 2008, pp. 192–213